A

B

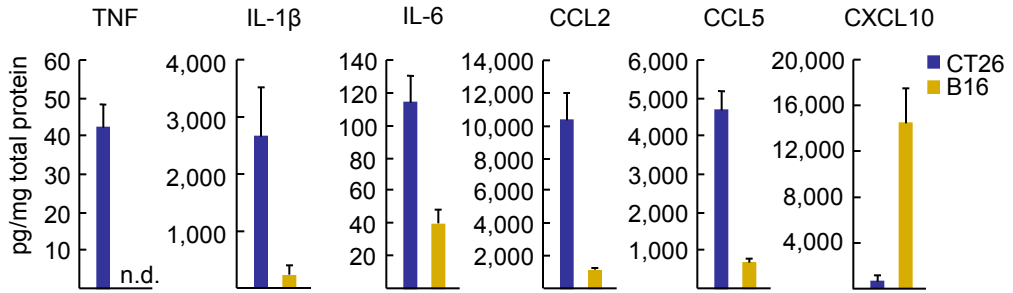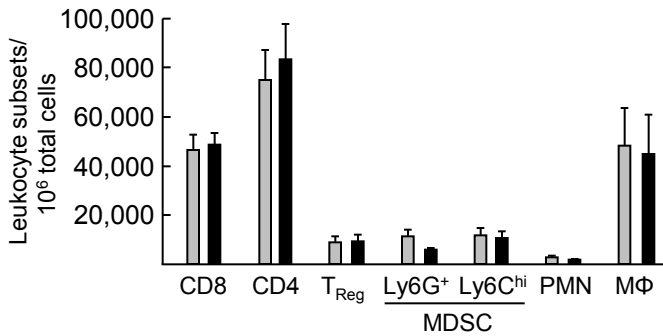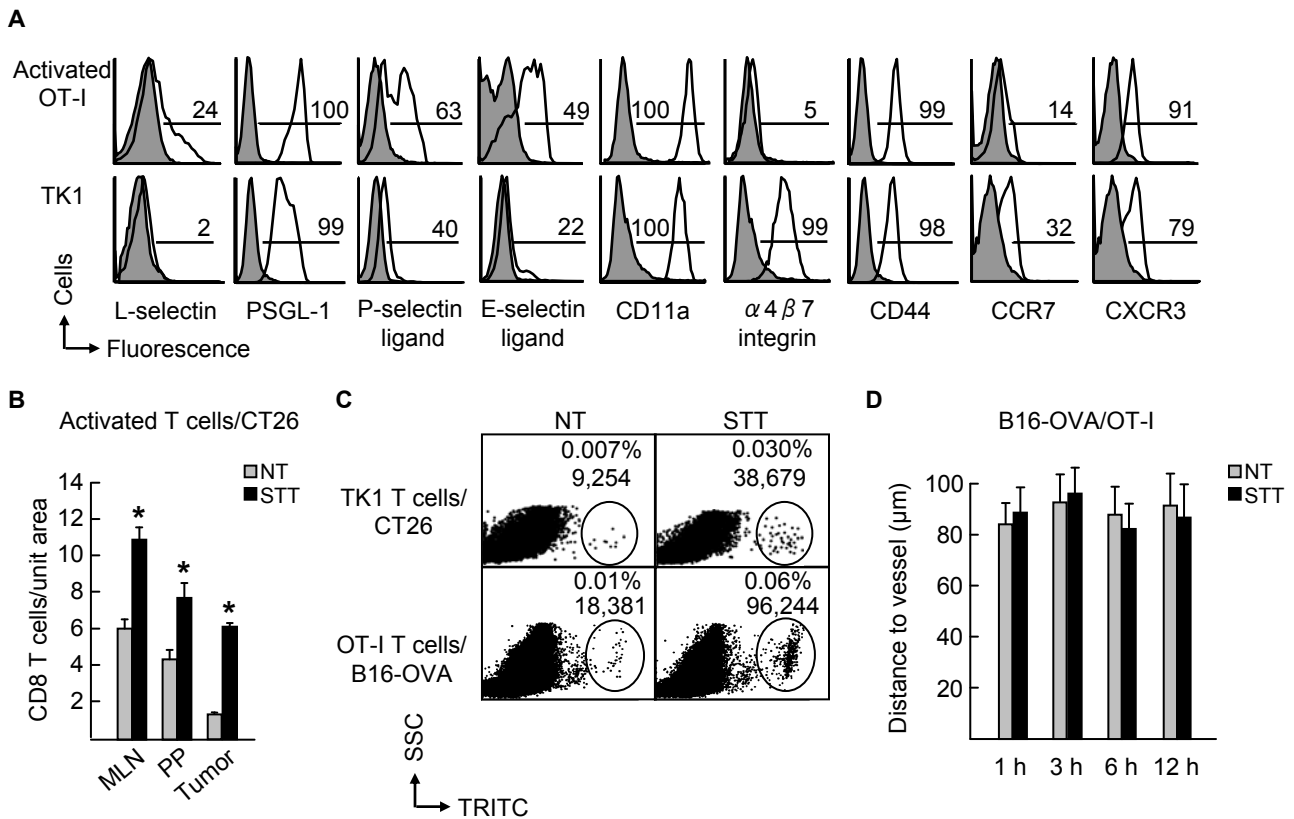**Supplemental Figure 1**

Cytokine expression in the tumor microenvironment and profile of leukocyte subsets in the spleen. (**A**) Expression of cytokines and chemokines in the tumor microenvironment of CT26 and B16 tumors measured by ELISA and Luminex. Data are for 3-6 mice per group; n.d., not detected. (**B**) Infiltration of leukocyte subsets in spleen from normothermic and STT-treated mice bearing B16-OVA tumors. Data are averages from 5 independent experiments; spleens from 3 mice/group were pooled and data were normalized to 10^6 total cells in each experiment. Comparison of NT and STT was not significant for any group.

A

	L-selectin	PSGL-1	P-selectin ligand	E-selectin ligand	CD11a	$\alpha 4 \beta 7$ integrin	CD44	CCR7	CXCR3
Activated OT-I	24	100	63	49	100	5	99	14	91
TK1	2	99	40	22	100	99	98	32	79

B Activated T cells/CT26
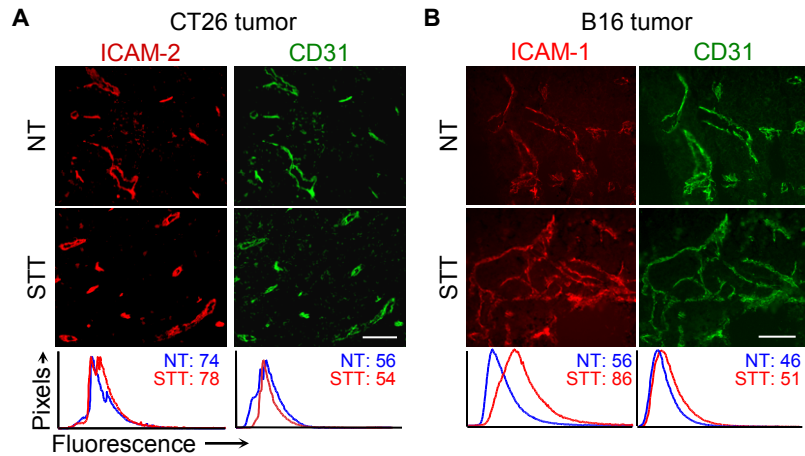
C

D B16-OVA/OT-I

Supplemental Figure 2

Homeostatic and thermally-inducible trafficking of CD8 T cells at different organ sites. (**A**) Representative histograms from flow cytometric analysis of adhesion molecule expression by activated OT-I cells or TK1 cells prior to adoptive transfer. Isotype control antibodies are grey histograms. CD11a is the α chain of LFA-1 integrin (the binding partner of ICAM-1). Numbers above bracketed lines indicate percent positive cells. (**B**) CD8 T cells isolated from lymph nodes draining subcutaneously implanted CT26 tumors were activated and expanded in vitro, labeled with TRITC, and injected intravenously (2 x 10^7 cells per mouse). Tissues were harvested 1 h after T cell transfer and TRITC-labeled cells were quantified by fluorescence microscopy. *, p < 0.01, NT versus STT. (**C**) TRITC-labeled CD8 T cells were injected i.v. (5 x 10^7 cells in CT26-bearing mice; 2 x 10^7 in B16-OVA-bearing mice) in tumor-bearing mice. After 1 h tumors were harvested and analyzed using flow cytometry. Data are pooled samples, n = 5 mice; shown are the percentage of total cells that were TRITC+ and the absolute number of TRITC+ CD8 T cells detected per tumor. SSC, side scatter. Data are representative of ≥ 3 independent

experiments. (**D**) The distance between adoptively transferred OT-I cells and the nearest CD31$^+$ vessels was measured using fluorescent microscopy. Data are representative of 2 independent experiments.

| T cells/ Mice	Tissues	Treatment	No. vessels	Vessel diameter (µm)	Blood cell velocity (µm)	Wall shear rate (s^{-1})
TK1/ BALB/c	Skin	NT	98	12.5 ± 0.6	276 ± 56	206 ± 77
		STT	112	12.9 ± 0.6	263 ± 71	236 ± 43
		LPS	89	13.2 ± 0.7	298 ± 87	235 ± 82
	CT26	NT	107	14.3 ± 0.6	236 ± 67	193 ± 81
		STT	109	13.5 ± 0.5	256 ± 74	171 ± 40
		LPS	126	14.5 ± 0.8	242 ± 76	181 ± 72
OT-I/ C57BL/6	Skin	NT	78	11.2 ± 0.7	309 ± 78	240 ± 91
		STT	89	12.6 ± 0.8	254 ± 92	182 ± 75
		LPS	93	11.7 ± 0.6	230 ± 96	226 ± 72
	B16-OVA	NT	86	13.2 ± 0.8	284 ± 84	192 ± 94
		STT	97	12.4 ± 0.9	310 ± 76	210 ± 80
		LPS	92	13.1 ± 0.8	264 ± 67	197 ± 92

Supplemental Figure 3

Vascular parameters in normal skin vessels and tumor vessels. The lumenal cross-sectional diameter of all analyzed vessels was measured in off-line observations. The velocity of ~10 non-interacting calcein-labeled T cells was measured and the wall shear rate was calculated. Data are from ≥ 3 independent experiments. There was no statistical difference between treatment groups ($p > 0.3$); n = 3 mice per group.

A CT26 tumor — ICAM-2 / CD31

NT / STT

Pixels → / Fluorescence →

NT: 74 / STT: 78

NT: 56 / STT: 54

B B16 tumor — ICAM-1 / CD31

NT / STT

NT: 56 / STT: 86

NT: 46 / STT: 51

Supplemental Figure 4

Thermal stress increases the expression of ICAM-1, but not ICAM-2, on tumor microvessels. (**A**) Control or STT-treated mice bearing subcutaneous CT26 tumors were injected intravenously with ICAM-2–specific antibody. Tumor cryosections were stained with TRITC-labeled secondary antibody to detect ICAM-2 (red) and counterstained with CD31-specific antibody (green) to demark vessels. (**B**) Immunofluorescence staining of ICAM-1 and CD31 in B16 tumors seeded in the lung. Histograms represent quantitative image analysis of the immunofluorescence intensity of adhesion molecules in CD31$^+$ vessels; numbers are MFI. Data are representative of ≥ 3 independent experiments. Scale bars, 50 µm.
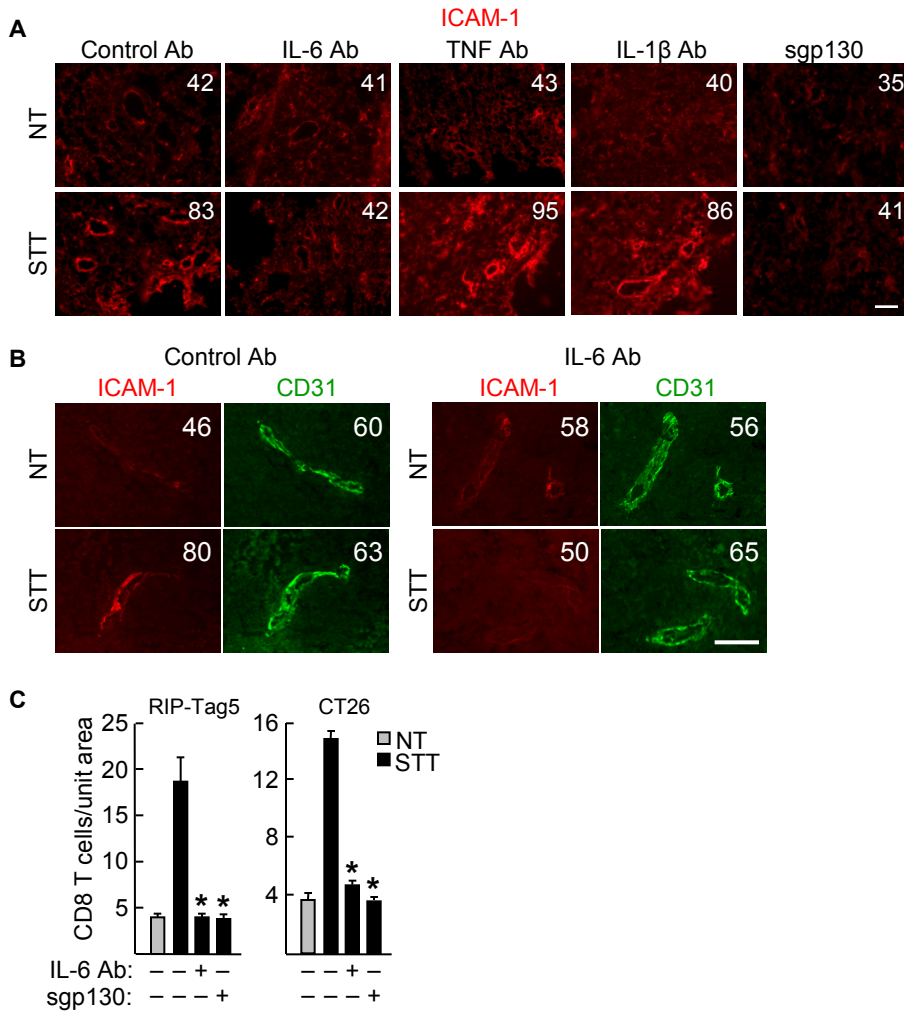
Supplemental Figure 5

Thermal stimulation of ICAM-1 is mediated by an IL-6 trans-signaling mechanism. Mice bearing CT26 tumors (**A**) or B16-OVA tumors (**B**) were treated with the indicated cytokine-blocking reagents. Tumor tissues were stained for ICAM-1 (red) and CD31 (green). Photomicrographs depict representative regions; numbers denote the MFI for all vessels. Scale bar, 50 µm. (**C**) Quantification of endogenous CD8 T cells in CT26 and RIP-Tag5 tumors. Data are representative of ≥ 3 independent experiments. *, $p < 0.0001$, function-blocking reagent versus STT.
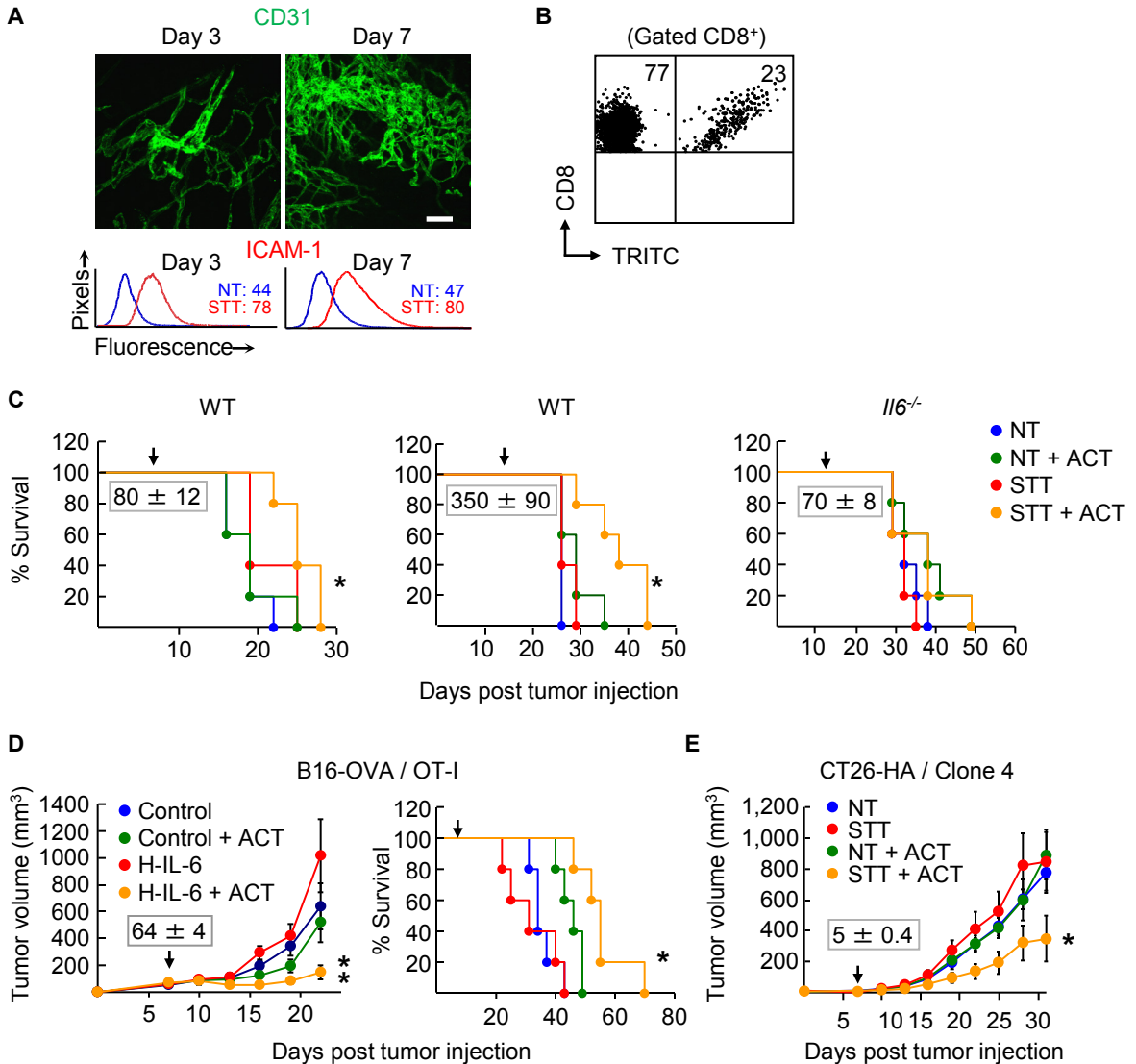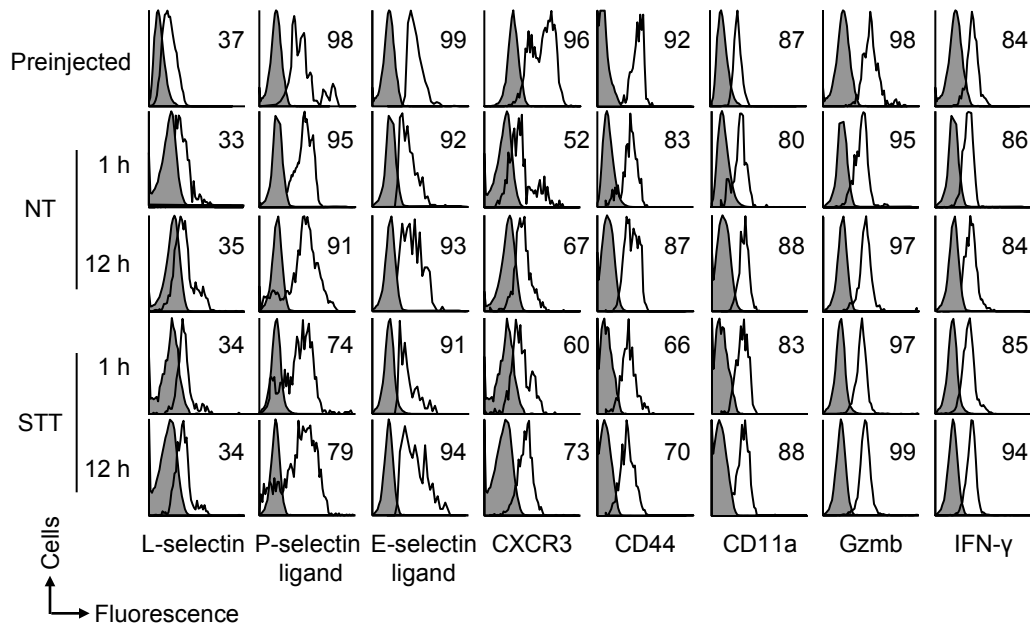
Supplemental Figure 6

Systemic thermal therapy in combination with adoptive cell therapy delays tumor growth.

(**A**) Photomicrographs depict vasculature of 3 or 7 day B16-OVA tumors shown by whole mount staining of CD31 and imaged using confocal microscopy. Intratumoral localization of vessels was confirmed by detection of melanin in bright field microscopy (not shown). Histograms show ICAM-1 induction by STT on vessels in both 3 and 7 day B16-OVA tumors; numbers denote the MFI for all vessels. Scale bar, 100 μm. Data are representative of 2 independent experiments. (**B**) Characterization of adoptively transferred OT-I effector cells. TRITC-labeled OT-I cells (1 x 10^7 cells per mouse) were

injected intravenously into B16-OVA bearing mice. The percentage of CD8 T cells in circulation that were TRITC-positive was determined 2 min after adoptive cell transfer (ACT). Adoptively transferred OT-I cells comprised 23% of the total circulating CD8 T cell population. Data shown are pooled samples (n=5 mice) gated on CD8+ cells and are representative of 3 independent experiments. (**C**) Survival curves of mice treated with STT and ACT of OT-1 effector T cells. (**D**) Left, tumor growth curves, and survival curves of mice bearing B16-OVA tumors treated with H-IL-6 ACT of OT-1 effector T cells. (**E**) Tumor growth curves of CT26-HA tumors in mice treated with STT and ACT of clone 4 effector T cells. (**C**-**E**) Time of STT and ACT treatment is indicated by arrow. Number in grey box is tumor volume (mm^3) at time of treatment. Data are from 5 mice for each condition and represent ≥ 2 independent experiments *, p < 0.006, **, p < 0.04, compared to normothermic control with adoptive transfer.

Supplemental Figure 7

Activated OT-I T cells that traffic into the tumor microenvironment display phenotype consistent with effector T cells. Representative histograms from flow cytometric analysis of the phenotype of activated OT-I cells prior to injection and in tumor tissues 1 h and 12 h after adoptive transfer. Numbers indicate percent positive cells; isotype control antibodies are grey histograms. CD11a is the α chain of LFA-1; Gzmb, granzyme B.

Supplemental Video 1

Adhesive interactions between TK1 CD8 T cells and CT26 tumor vessels are limited under normothermic conditions.

Supplemental Video 2

STT increases rolling interactions and firm sticking of TK1 CD8 T cells within CT26 tumor vessels.

Supplemental Video 3

E/P-selectin blocking antibodies abrogate thermally-induced TK1 CD8 T cell rolling interactions in CT26 tumor microvessels.

Supplemental Video 4

Functional blockade of G-protein coupled chemokine receptors by pertussis toxin inhibits firm sticking of TK1 CD8 T cells in CT26 tumor microvasculature in STT-treated mice.

Supplemental Video 5

ICAM-1 neutralizing antibody blocks STT-induced firm sticking of TK1 CD8 T cells in CT26 tumor vessels.

Supplemental Methods

Animals. Female mice were from the National Cancer Institute, Jackson Laboratory or Taconic: BALB/c, C57BL/6, IL-6–deficient (B6.129S2-Il6tm1Kopf/J on a C57BL/6 background), and ICAM-1–deficient (Icam1tmJegr/J on a C57BL/6 background). OT-I mice (C57BL/6-Tg(TcraTcrb)1100Mjb/J) were from Jackson Laboratory. RIP-Tag5 (RIP1-Tag5 on a C3HeB/Fe background; provided by Douglas Hanahan, UCSF, San Francisco, CA) and Clone 4 mice (CBy.Cg-*Thy1^a* Tg(Tcra(C14,TcrbC14)1Shrm/ShrmJ; from Linda Sherman, Scripps Research Institute, La Jolla, CA) were bred in the Roswell Park Department of Laboratory Animal Resources. Chimeric mouse models were generated by lethally irradiating host mice (10 Gy total in 2 doses, 3 h apart) followed by reconstitution with 1 x 10^6 donor bone marrow cells. After 9 weeks of recovery, mice were implanted subcutaneously with tumor cells.

Tumor models. 10^6 tumor cells (CT26, CT26-HA, B16/F10, B16/F10-OVA, or EMT6 cells) were injected subcutaneously in the flank of 8-10 week-old BALB/c or C57BL/6 mice and used for experimental analysis 2-3 weeks post-implantation unless otherwise indicated. Tumor cells (106 B16/F10 cells) were injected in the tail vein to model end-stage metastasis to the lungs. RIP-Tag5 mice were used at ~26 weeks of age.

Flow cytometry. Phenotypic analysis was performed by multiparameter flow cytometry of cell immunostained using the following monoclonal antibodies: anti-CD8α (53-6.7, PerCP), anti-CD4 (RM4-5, PerCP), anti-CD25 (PC61, APC), anti-FoxP3 (MF23, PE), anti-CD11b (1M/70, PE-Cy7), anti-Ly6C (AL-21, FITC), anti-Ly6G (1A8, PE), anti-L-selectin (Mel-14, APC), anti-PSGL1 (4RA10, FITC), anti-α4β7 integrin (DATK-32, PE), anti-CD44 (IM7, FITC),

anti-CD11a (2D7, FITC/PE) (BD Biosciences); anti-CXCR3 (220803, APC) (R&D Systems); anti-CCR7 (4B12, APC), anti-granzyme B (16G6, AF647), and anti-IFN-γ (XMG1.2, APC) (eBioscience). Functional P-selectin and E-selectin ligands were detected with CD62P or CD62E-IgG fusion proteins, respectively (R&D Systems).

Intravital microscopy. Vessels were visualized by a epi-illumination intravital microscope with a custom stage equipped with a warming pad and vibration dampening system (Spectra Services). All images were captured with an EB charge-coupled device camera (Hamamatsu Photonics) and recorded with a digital videocassette recorder (DSR-11; Sony) and quantified by observers blinded to treatment conditions. For these studies it was necessary to transfer supraphysiological numbers of CD8 T cells in order to track them in the observation field since most i.v. transferred cells are trapped in the lungs. However, similar adhesive interactions were observed regardless of the number transferred (i.e., $\sim 10^8$ TK1 cells and $\sim 2 \times 10^7$ OT-1 cells), suggesting that these assays accurately measured the adhesive capacity of CD8 effector T cells. Lumenal cross-sectional diameter (D) of vessels and velocity (V) of noninteracting calcein-labeled cells were measured in off-line observations (15, 17). Wall shear rate (γ) was calculated as $8(V \div D)$ (20).

Immunohistochemistry and immunofluorescence histology. Deparaffinized tumor sections (9 μm-thick) were blocked with Superblock Blocking Buffer (Pierce) and stained with anti-CD8 antibody (53-6.7, BD Biosciences). Biotinylated secondary antibodies (Jackson ImmunoResearch) were detected using the VectaStain ABC substrate kit (Vector Laboratories).

For immunofluorescence studies, OCT (Sakura Finetek)-embedded tissue cryosections (9 µm-thick) were fixed at -20°C in methanol/acetone (3:1), blocked using 10% serum, and stained with primary antibodies (polyclonal anti-phospho-STAT3 antibody (Santa Cruz), polyclonal anti-gp130 antibody (R&D Systems), or anti-mouse CD31 antibody (MEC 13.3, BD Biosciences)). Patient tumor cryosections were stained using anti-human ICAM-1 antibody (LB-2, BD Biosciences) and anti-human CD31 antibody (polyclonal, Abcam). For intravascular staining, azide and endotoxin-free primary antibody specific for ICAM-1 (3E2, 50 µg/mouse), ICAM-2 (3C4, 50 µg/mouse) (BD Biosciences), or isotype controls were injected via the tail vein and organs were collected after 20 min as described (16, 30). After staining with fluorochrome-conjugated secondary antibody (Jackson ImmunoResearch), specimens were mounted in Aqua Poly/Mount (Polysciences, Inc.) or Vectashield with DAPI (Vector Laboratories). Pilot studies confirmed that comparable results were obtained by intravascular and tissue-section staining. Moreover, coincident staining was detected in 98% of vessels using the pan-endothelial adhesion molecules CD31 (by tissue-section staining) and ICAM-2 (intravascular staining), validating that the majority of tumor vessels were accessible to detection antibodies in vivo. Whole tumor mounts were stained with anti-CD31 antibody (MEC 13.3, FITC; BD Biosciences) for 1.5 h followed by a 5 h wash. 40 µm-thick optical sections were imaged using a Leica TCS SP2 Spectral confocal microscope.